Synthesis and reactivities of Ir₂Ru heterobimetallic sulfido clusters derived from a hydrogensulfido-bridged diiridium complex

Takuya Kochi,[a] Yasuo Nomura,[a] Zhen Tang,[a] Youichi Ishii,[a] Yasushi Mizobe[b] and Masanobu Hidai *[a]

[a] Department of Chemistry and Biotechnology, Graduate School of Engineering, The University of Tokyo, Hongo, Bunkyo-ku, Tokyo 113-8656, Japan
[b] Institute of Industrial Science, The University of Tokyo, Roppongi, Minato-ku, Tokyo 106-8558, Japan. E-mail: hidai@chembio.t.u-tokyo.ac.jp

The hydrogensulfido-bridged diiridium complex [ClCp*Ir(μ-SH)₂IrCp*Cl] reacted with [RuH₂(PPh₃)₄] to give a mixed-metal trinuclear cluster with an Ir₂Ru(μ₃-S)₂ core [(Cp*Ir)₂(μ₃-S)₂RuCl₂(PPh₃)] **2**, which was further converted into the cationic diphosphine derivatives [(Cp*Ir)₂(μ₃-S)₂RuCl(L)]Cl (L = dppe = Ph₂PCH₂CH₂PPh₂ **3** or depe = Et₂PCH₂CH₂PEt₂ **4**). The reaction of cluster **3** with Me₂CuLi followed by anion metathesis with KPF₆ afforded the cationic methyl cluster [(Cp*Ir)₂(μ₃-S)₂RuMe(dppe)][PF₆] **5** in good yield, while treatment of **3** with CHCl₂Li led to selective formation of [(Cp*Ir){(η⁴-C₅Me₅CHCl₂)Ir}(μ₃-S)₂RuCl(dppe)] **6**, in which one of the Cp* ligands was alkylated by CHCl₂Li to form an η⁴-diene. Clusters **3** and **4** were also transformed into the dihydrido clusters [(Cp*Ir)₂(μ₃-S)₂(μ-H)₂Ru(L)] (L = dppe **7** or depe **8**) by the reaction with NaBH₄. On the other hand, cluster **2** was converted into the carbonyl cluster [(Cp*Ir)₂(μ₃-S)₂RuCl(CO)(PPh₃)]Cl **9**, the isocyanide clusters [(Cp*Ir)₂-(μ₃-S)₂RuCl(CNXy)(PPh₃)]Cl **10** (Xy = 2,6-C₆H₃Me₂) and [(Cp*Ir)₂(μ₃-S)₂Ru(CNXy)₂(PPh₃)][BPh₄]₂ **11** and the co-ordinatively unsaturated thiolato clusters [(Cp*Ir)₂(μ₃-S)₂Ru(SAr)₂] (Ar = 2,4,6-C₆H₂Pr^i₃ **12** or Xy **13**) on treatment with CO, XyNC and LiSAr, respectively. The molecular structures of [(Cp*Ir)₂(μ₃-S)₂RuCl(depe)][BPh₄] **4′**, **5**·CH₂Cl₂, **6**, **7** and **12**·2C₆H₆ were established by X-ray diffraction studies.

Transition-metal complexes with sulfur-based ligands have been attracting increasing interest,[1] primarily because they serve as models for biological systems[2] and industrial metal sulfide catalysts.[3] Complexes of metals relevant to such systems, most typically those of iron and molybdenum, have been extensively investigated. In contrast, the chemistry of noble metal complexes with sulfur ligands still remains much less exploited. With the intention of developing complexes with robust and reactive multimetallic sites, we have synthesized several types of multinuclear Group 8–10 noble metal complexes with sulfido or thiolato ligands.[4] In fact, intriguing transformations of various substrate molecules have been achieved on the multimetallic centres of, for example, [Cp*RuCl(μ-SPr^i)₂Ru(OH₂)Cp*]-[O₃SCF₃][5] (Cp* = η⁵-C₅Me₅) and [PdMo₃(μ₃-S)₄(tacn)₃Cl]-[PF₆]₃[6] (tacn = 1,4,7-triazacyclononane).[6] Inspired by these results, we have embarked on establishing a general and rational route for the construction of noble metal sulfido clusters with designed structures. Recently, we have newly synthesized a series of hydrogensulfido complexes [ClCp*M(μ-SH)₂MCp*Cl] (M = Ru,[7] Rh[8] or Ir[8]) and [Cp₂Ti(μ-SH)₂RuCp*Cl] (Cp = η⁵-C₅H₅),[4d] and found that they can be used as versatile precursors for the syntheses of homo- and hetero-metallic sulfido clusters.[4c–e,7,8] In particular, the hydrogensulfido complex of iridium [ClCp*Ir(μ-SH)₂IrCp*Cl] **1** is transformed into various heterobimetallic clusters including trinuclear clusters with the triangular Ir₂M(μ₃-S)₂ core (M = Rh,[8a] Pd,[8a,c] Pt[8c] or Fe[4e]) and pentanuclear clusters with the bow-tie type Ir₄M(μ₃-S)₄ core (M = Fe, Co or Ni)[4e] by reaction with a second metal fragment. In addition, the trinuclear cluster [(Cp*Ir)₂(μ₃-S)₂PdCl₂] derived from **1** exhibits unique regioselectivity in the addition of alcohols to internal 1-aryl-1-alkynes.[8c] Now we have synthesized mixed-metal trinuclear clusters with an Ir₂Ru(μ₃-S)₂ core [(Cp*Ir)₂(μ₃-S)₂RuCl₂(PPh₃)] **2** and [(Cp*Ir)₂(μ₃-S)₂RuCl(L)]Cl (L = dppe = Ph₂PCH₂CH₂PPh₂ **3** or depe = Et₂PCH₂CH₂PEt₂

4) from complex **1**. Clusters **2**, **3** and **4** displayed interesting reactivities including regioselective alkylation of **3** either at the ruthenium centre or at the Cp* ligand.

Results and discussion

Preparation of the trinuclear cluster [(Cp*Ir)₂(μ₃-S)₂RuCl₂-(PPh₃)] 2 and its diphosphine derivatives 3 and 4

Reaction of complex **1** with an almost equimolar amount of [RuH₂(PPh₃)₄] in thf smoothly took place at room temperature to give the mixed-metal trinuclear cluster **2** in good yield, eqn. (1). Evolution of H₂ gas (1.44 mol per **1**) during the


$$+ [RuH_2(PPh_3)_4] \tag{1}$$
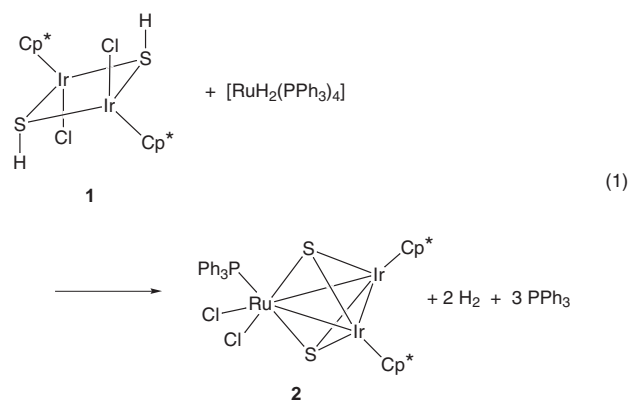
reaction was confirmed by GLC analysis of the gaseous phase, suggesting that two molecules of H₂ were formed per one of cluster **2**. As a related reaction, we have recently reported that the diruthenium complex [ClCp*Ru(μ-SH)₂RuCp*Cl] reacts with [RuH₂(PPh₃)₄] to give a triruthenium cluster with a

bridging hydrido ligand [(Cp*Ru)$_2$(μ_3-S)$_2$(μ-H)RuCl(PPh$_3$)$_2$].[4c] In the present reaction, however, cluster **2** was essentially the sole product detected by the ^{1}H NMR analysis of the crude reaction mixture, and formation of hydrido clusters was not observed. Cluster **2** could also be prepared from **1** and [RuCl$_2$(PPh$_3$)$_3$], but the reaction was sluggish (23% conversion after 2 d at room temperature).

Cluster **2** was characterized by its ^{1}H and ^{31}P-{^{1}H} NMR spectra as well as the crystallographic study of its depe derivative described below. At room temperature, the ^{1}H NMR spectrum exhibited one Cp* singlet (δ 1.95) and aromatic signals due to the PPh$_3$ ligand with the intensity ratio of 2:1, while the ^{31}P-{^{1}H} NMR signal appeared as a broad singlet at δ 82.9. On lowering the temperature to −60 °C the Cp* signal in the ^{1}H NMR split into two singlets at δ 1.64 and 2.19 with the same intensities. This NMR behavior indicates that the favored conformer of the cluster at low temperatures has an unsymmetric structure where the PPh$_3$ ligand is located out of the RuS$_2$ plane, but the co-ordination around the ruthenium atom is fluxional at room temperature to make the two Cp* ligands apparently equivalent.

The Ir$_2$RuS$_2$ cluster core was further characterized as diphosphine derivatives. Thus, on treatment with dppe or depe, cluster **2** was converted into the cationic cluster **3** or **4**, respectively (Scheme 1), and the molecular structure of [(Cp*Ir)$_2$-
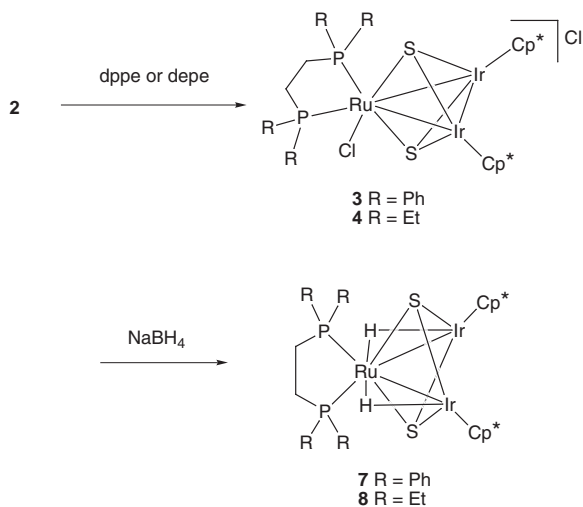
Scheme 1

(μ$_3$-S)$_2$RuCl(depe)][BPh$_4$] **4′**, the [BPh$_4$]$^-$ analogue of **4**, was unequivocally established by X-ray analysis. An ORTEP[9] drawing of the cation in **4′** is illustrated in Fig. 1, and selected bond distances and angles are listed in Table 1. Cluster **4′** has a triangular Ir$_2$Ru core capped by two μ$_3$-sulfido ligands from both sides. The two Ir–Ru contacts at 2.8922(9) and 2.8437(9) Å and the Ir–Ir contact at 2.7848(6) Å are consistent with Ir–Ru[10] and Ir–Ir[4e,11] single bonds, respectively. The Ru(1) atom is further co-ordinated by a chelating depe molecule and a chloro ligand, and if the two Ir–Ru bonds are neglected the geometry around the ruthenium atom is distorted trigonal bipyramidal with the S(1) and P(2) atoms at the apical positions. This geometry makes the molecule unsymmetric as a whole. The Ru(1)–S(1) distance [2.332(3) Å] is appreciably longer than Ru(1)–S(2) [2.261(3) Å] probably due to the *trans* influence of the P(2) atom. Although several Ir$_3$(μ$_3$-S)$_2$[11c,d] and Ru$_3$(μ$_3$-S)$_2$[4c,12] clusters with related structures have been reported, the mixed-metal Ir$_2$Ru(μ$_3$-S)$_2$ core is unprecedented.

At room temperature, each of complexes **3**, **4** and **4′** showed one Cp* signal (δ 1.88 for **3**; 2.11 for **4**; 1.99 for **4′**) in the ^{1}H NMR spectrum, although the cation in **4′** takes the unsymmetric solid state structure as described above. Their ^{31}P-{^{1}H} NMR spectra also displayed only one sharp singlet (δ 81.0 for **3**; 82.3 for **4** and **4′**). Furthermore, in contrast to cluster **2**, these
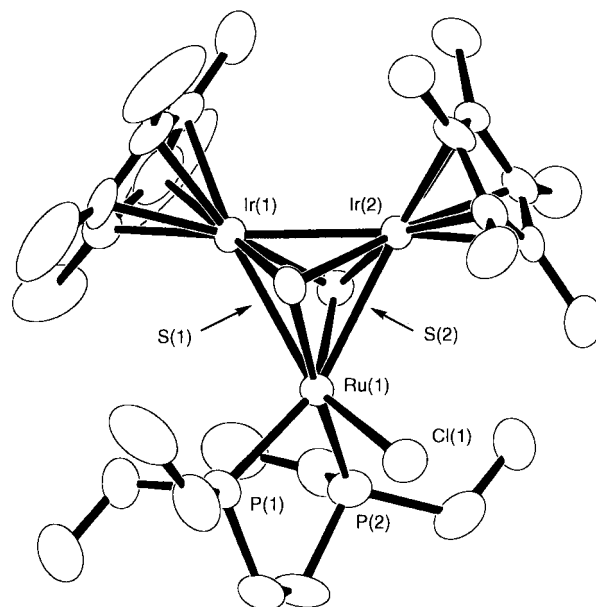
Fig. 1 Structure of the cationic part in complex **4′**. Hydrogen atoms are omitted for clarity. Thermal ellipsoids are shown at the 50% probability level.

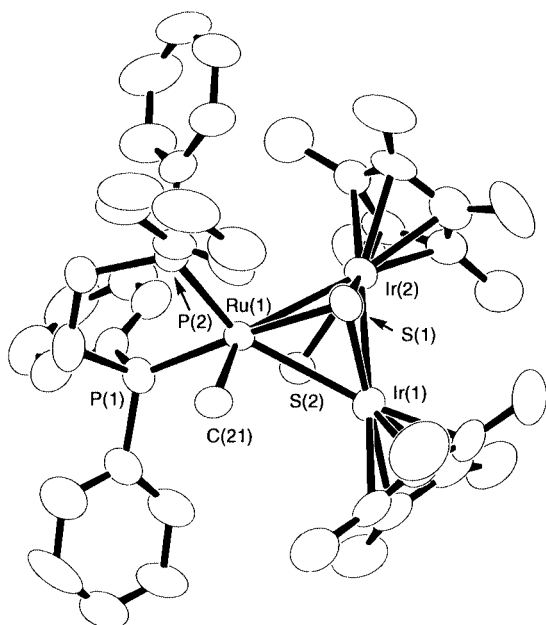**Table 1** Selected interatomic distances (Å) and angles (°) in complex **4′**

Ir(1)–Ir(2)	2.7848(6)	Ir(1)–Ru(1)	2.8922(9)
Ir(2)–Ru(1)	2.8437(9)	Ir(1)–S(1)	2.285(3)
Ir(1)–S(2)	2.277(3)	Ir(2)–S(1)	2.291(3)
Ir(2)–S(2)	2.290(3)	Ru(1)–Cl(1)	2.392(3)
Ru(1)–S(1)	2.332(3)	Ru(1)–S(2)	2.261(3)
Ru(1)–P(1)	2.295(3)	Ru(1)–P(2)	2.313(3)
Ir(2)–Ir(1)–Ru(1)	60.08(2)	Ir(1)–Ir(2)–Ru(1)	61.83(2)
Ir(1)–Ru(1)–Ir(2)	58.08(2)	S(1)–Ir(1)–S(2)	88.90(9)
S(1)–Ir(2)–S(2)	88.41(9)	Cl(1)–Ru(1)–S(1)	91.80(10)
Cl(1)–Ru(1)–S(2)	134.8(1)	S(1)–Ru(1)–S(2)	88.11(9)
S(1)–Ru(1)–P(1)	101.5(1)	S(1)–Ru(1)–P(2)	176.9(1)
S(2)–Ru(1)–P(1)	139.4(1)	S(2)–Ru(1)–P(2)	89.7(1)

cationic clusters exhibited no notable temperature dependence in the ^{1}H NMR spectra. Therefore, the cationic clusters **3** and **4** are considered to be much more fluxional than **2** with respect to the geometry around the ruthenium atom.

Regioselective alkylation reactions of cluster 3

Alkylation of cluster **3** was examined in detail. Although its reactions with MeLi, PhLi and MeMgBr ended in the formation of complex mixtures, selective methylation of the ruthenium centre was achieved by the reaction with Me$_2$CuLi at −20 °C. The ^{1}H NMR analysis of the crude product indicated the formation of a single cluster species, and the cationic methyl cluster [(Cp*Ir)$_2$(μ$_3$-S)$_2$RuMe(dppe)][PF$_6$]·CH$_2$Cl$_2$ **5**·CH$_2$Cl$_2$ was isolated in 67% yield after anion metathesis with KPF$_6$ (Scheme 2). The ^{1}H NMR spectrum of cluster **5** exhibited one triplet at δ −1.14 [3 H, ^3J(PH) = 6.4 Hz] assignable to the RuMe protons and one singlet at δ 1.85 (30 H) due to the Cp* protons, both of which are consistent with the formulation. Attempted methylation of cluster **2** with Me$_2$CuLi did not give any isolable methyl clusters.
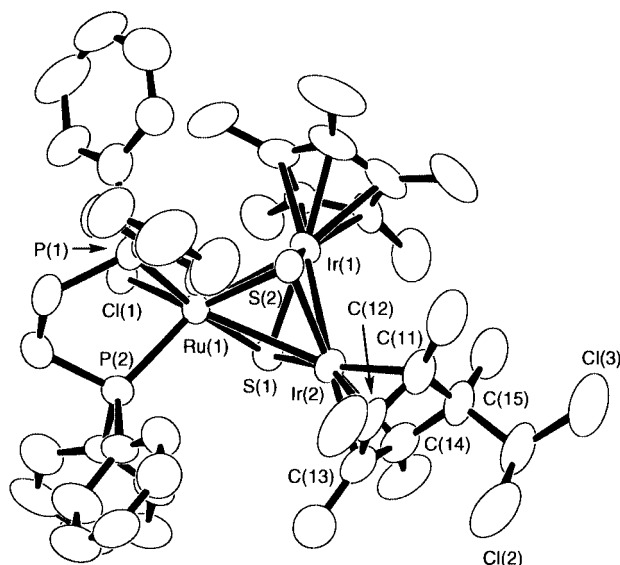
The molecular structure of complex **5**·CH$_2$Cl$_2$ was determined by X-ray analysis. An ORTEP drawing of the cation is given in Fig. 2, and important bond distances and angles are in Table 2. Cluster **5** has a triangular Ir$_2$Ru core capped by two μ$_3$-sulfido ligands, which is closely related to that of **4′**. The three metal–metal distances [Ir(1)–Ir(2), 2.7717(5); Ir(1)–Ru(1), 2.8695(8); Ir(2)–Ru(1), 2.978(1) Å] are diagnostic of metal–metal bonding interactions, where the elongation of the Ir(2)–Ru(1) bond is attributed to the steric congestion between the

Fig. 2 Structure of the cationic part in complex **5·CH₂Cl₂**. Details as in Fig. 1.

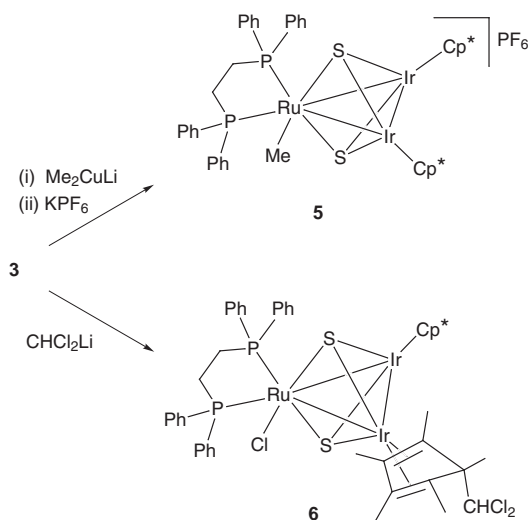**Table 2** Selected interatomic distances (Å) and angles (°) in complex **5·CH₂Cl₂**

Ir(1)–Ir(2)	2.7717(5)	Ir(1)–Ru(1)	2.8695(8)
Ir(2)–Ru(1)	2.978(1)	Ir(1)–S(1)	2.284(3)
Ir(1)–S(2)	2.273(2)	Ir(2)–S(1)	2.288(2)
Ir(2)–S(2)	2.276(2)	Ru(1)–S(1)	2.328(2)
Ru(1)–S(2)	2.295(2)	Ru(1)–P(1)	2.266(3)
Ru(1)–P(2)	2.277(3)	Ru(1)–C(21)	2.147(9)
Ir(2)–Ir(1)–Ru(1)	63.71(2)	Ir(1)–Ir(2)–Ru(1)	59.74(2)
Ir(1)–Ru(1)–Ir(2)	56.55(2)	S(1)–Ir(1)–S(2)	87.70(9)
S(1)–Ir(2)–S(2)	87.52(8)	S(1)–Ru(1)–S(2)	86.10(9)
S(1)–Ru(1)–P(1)	176.05(10)	S(1)–Ru(1)–P(2)	100.24(9)
S(1)–Ru(1)–C(21)	95.4(3)	S(2)–Ru(1)–P(1)	91.75(9)
S(2)–Ru(1)–P(2)	146.86(9)	S(2)–Ru(1)–C(21)	125.9(3)

Scheme 2

phenyl groups on the P(2) atom and the Cp* ligand on the Ir(2) atom. It has unambiguously been confirmed that a methyl ligand [C(21)] is introduced onto the ruthenium centre. The geometry around the Ru(1) atom is distorted trigonal bipyramidal with the P(1) and S(1) atoms at the apical positions and the P(2), S(2) and C(21) atoms on the basal plane.

In contrast, treatment of cluster **3** with CHCl₂Li led to formation of [(Cp*Ir){(η⁴-C₅Me₅CHCl₂)Ir}(μ₃-S)₂RuCl(dppe)]

Fig. 3 Molecular structure of complex **6**. Details as in Fig. 1.

Table 3 Selected interatomic distances (Å) and angles (°) in complex **6**

Ir(1)–Ir(2)	2.8604(5)	Ir(1)–Ru(1)	2.8199(9)
Ir(2)–Ru(1)	2.9740(9)	Ir(1)–S(1)	2.294(2)
Ir(1)–S(2)	2.278(2)	Ir(2)–S(1)	2.285(2)
Ir(2)–S(2)	2.274(2)	Ir(2)–C(11)	2.159(10)
Ir(2)–C(12)	2.128(10)	Ir(2)–C(13)	2.13(1)
Ir(2)–C(14)	2.16(1)	Ru(1)–Cl(1)	2.428(2)
Ru(1)–S(1)	2.363(3)	Ru(1)–S(2)	2.296(2)
Ru(1)–P(1)	2.287(3)	Ru(1)–P(2)	2.274(3)
C(11)–C(12)	1.43(1)	C(11)–C(15)	1.52(1)
C(12)–C(13)	1.46(1)	C(13)–C(14)	1.41(1)
C(14)–C(15)	1.55(1)		
Ir(2)–Ir(1)–Ru(1)	63.14(2)	Ir(1)–Ir(2)–Ru(1)	57.77(2)
Ir(1)–Ru(1)–Ir(2)	59.10(2)	S(1)–Ir(1)–S(2)	87.61(8)
S(1)–Ir(2)–S(2)	87.92(9)	Cl(1)–Ru(1)–S(1)	89.33(8)
Cl(1)–Ru(1)–S(2)	136.12(9)	S(1)–Ru(1)–S(2)	85.55(8)
S(1)–Ru(1)–P(1)	173.32(9)	S(1)–Ru(1)–P(2)	103.44(9)
S(2)–Ru(1)–P(1)	90.71(9)	S(2)–Ru(1)–P(2)	141.38(10)
C(12)–C(11)–C(15)	108(1)	C(11)–C(12)–C(13)	106.0(10)
C(12)–C(13)–C(14)	107(1)	C(13)–C(14)–C(15)	108.0(9)
C(11)–C(15)–C(14)	95.5(8)		

6, which was isolated as dark brown crystals in 57% yield (Scheme 2). Formation of no other cluster species was observed by the ¹H NMR analysis of the crude reaction mixture, indicating that cluster **6** was produced quite selectively. The ¹H NMR spectrum of cluster **6** showed a set of singlets at δ 1.21 (3 H), 1.79 (6 H), 1.95 (6 H) and 5.23 (1 H) due to the η⁴-C₅Me₅CHCl₂ ligand, which revealed that one of the Cp* ligands in **3** was alkylated by CHCl₂Li to form the substituted η⁴-cyclopentadiene ligand. This type of conversion of a Cp* ligand into a substituted η⁴-cyclopentadiene ligand has been relatively rare.[13] Very recently, Tanaka *et al.*[13c] have reported that the trinuclear cluster [(Cp*Ir)₃(μ₃-S)₂], which is generated by electrochemical reduction of [(Cp*Ir)₃(μ₃-S)₂][BPh₄]₂, reacts with MeCN under CO₂ to give a cationic cluster with a substituted η⁴-cyclopentadiene ligand [(Cp*Ir)₂{(η⁴-C₅Me₅CH₂-CN)Ir}(μ₃-S)₂][BPh₄], although the reaction mechanism has not been clarified.

The molecular structure of cluster **6** was further confirmed by X-ray diffraction study. An ORTEP drawing is illustrated in Fig. 3, and selected bond distances and angles are contained in Table 3. The metric features of the Ir₂Ru(μ₃-S)₂ core in **6** are similar to those found in **5·CH₂Cl₂** except that the Ir(1)–Ir(2) bond in **6** [2.8604(5) Å] is elongated. The η⁴ co-ordination of the newly formed C₅Me₅CHCl₂ ligand with the Ir(2)–C bond distances at 2.128(10)–2.16(1) Å has been confirmed. The Ir(2) atom is now co-ordinated by the two sulfur atoms and the diene

ligand with a square planar geometry. This structure suggests that the Ir(2) atom is reduced to the formal oxidation state of Ir^I on reaction with CHCl$_2$Li. On the other hand, the structure around the ruthenium atom is trigonal bipyramidal and closely related to that of cluster 4′.

The diffraction study of complex 6 has also revealed that the CHCl$_2$ group in the η^4-C$_5$Me$_5$CHCl$_2$ ligand is located at the *exo* position. A mechanism consistent with the structure would involve direct nucleophilic attack of CHCl$_2$Li at the Cp* ligand in the cationic cluster 3 from the outer co-ordination sphere,[13a,b] since indirect attack of a CHCl$_2$ group *via* the iridium centre to the Cp* ring is expected to lead to the *endo* η^4-C$_5$Me$_5$CHCl$_2$ isomer.[14] Alternatively, a mechanism involving the coupling of a CHCl$_2$ radical and the neutral cluster [(Cp*Ir)$_2$(μ$_3$-S)$_2$-RuCl(dppe)] formed by one electron transfer between CHCl$_2$Li and 3 may be operative.[15] It should be pointed out that the reaction site of 3 attacked by an alkylmetal reagent is highly dependent upon the nature of the reagent. We consider that soft and sterically small alkylmetals are driven to attack the ruthenium centre, while sterically demanding alkylmetals tend to attack the Cp* ligand.

Preparation of dihydrido clusters from 3 and 4

The regioselective alkylation reactions observed with cluster 3 led us to investigate the reactions of 2, 3 and 4 with a hydride reagent for comparison. When cluster 3 was allowed to react with an excess amount of NaBH$_4$ in CH$_2$Cl$_2$–ethanol at room temperature the dihydrido cluster [(Cp*Ir)$_2$(μ$_3$-S)$_2$(μ-H)$_2$Ru-(dppe)] 7 was obtained in moderate yield (Scheme 1). Cluster 4 was analogously converted into the corresponding dihydrido cluster [(Cp*Ir)$_2$(μ$_3$-S)$_2$(μ-H)$_2$Ru(depe)] 8. However, no char-acterizable hydrido cluster was obtained from 2.

In the ^{1}H NMR spectrum cluster 7 exhibited a high-field hydrido resonance at δ −14.73 with the intensity of 2 H as a triplet by coupling with two equivalent phosphorus nuclei [^2J(PH) = 13.4 Hz] as well as one Cp* signal at δ 1.97 (30 H). No temperature dependence was observed for these signals over the range 20 to −80 °C. The ^{31}P-{^{1}H} NMR spectrum also showed only one singlet, confirming the apparent equivalence of the phosphorus nuclei. The IR spectrum had no absorption in the range 1500–2200 cm^{-1} attributable to a terminal M–H stretching. Considering these spectral data, cluster 7 is deduced to have two hydrido ligands which bridge the two respective Ru–Ir edges. Cluster 8 showed a hydrido signal at δ −14.56 as a triplet [^2J(PH) = 15.9 Hz] in the ^{1}H NMR spectrum but no IR absorption assignable to a terminal M–H stretching, revealing a structure similar to that of 7.

The molecular structure of complex 7 was established by X-ray analysis. The unit cell contains two independent mol-ecules, whose structures are essentially equivalent. An ORTEP drawing for one is depicted in Fig. 4, and important bond dis-tances and angles are collected in Table 4. The Ir–Ru distances at an average of 2.803 Å are shorter than those found in clusters 4′, 5·CH$_2$Cl$_2$ and 6 and suggest that there exists substantial metal–metal bonding character between the ruthenium and iridium atoms. Although the positions of the hydrido ligands could not be determined crystallographically, each of these Ir–Ru edges is considered to be bridged by a hydrido ligand on the basis of the above mentioned spectroscopic data. The geometry around the ruthenium atom is viewed as distorted octahedral with the mutually *trans* μ-hydrido ligands, if the Ru–Ir interactions are neglected. On the other hand, the Ir–Ir separation in each independent cluster molecule [3.509(1), 3.568(2) Å] is much longer than those of 4′, 5·CH$_2$Cl$_2$ and 6 and is regarded to be non-bonding. The loss of the Ir–Ir bond makes the Ir–Ru–Ir bond angle [77.26(6), 79.31(6)°] signi-ficantly larger than the corresponding values found in 4′, 5·CH$_2$Cl$_2$ and 6 [56.55(2)–59.10(2)°]. The structure with the two metal–metal bonding contacts is in good agreement with the 50
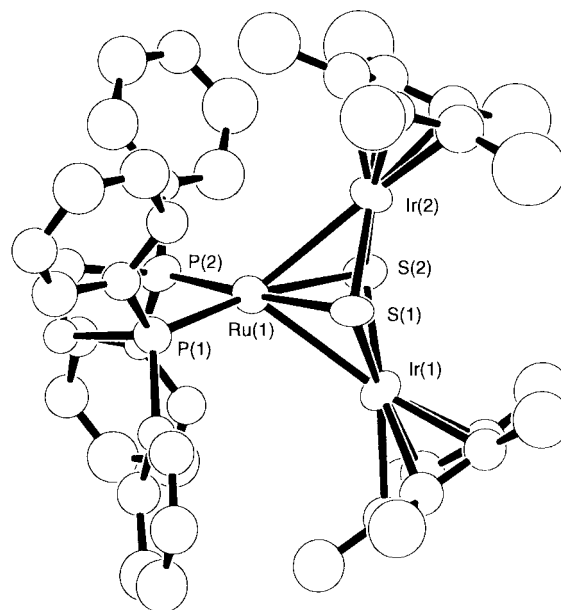

Fig. 4 Molecular structure of complex 7. Details as in Fig. 1.

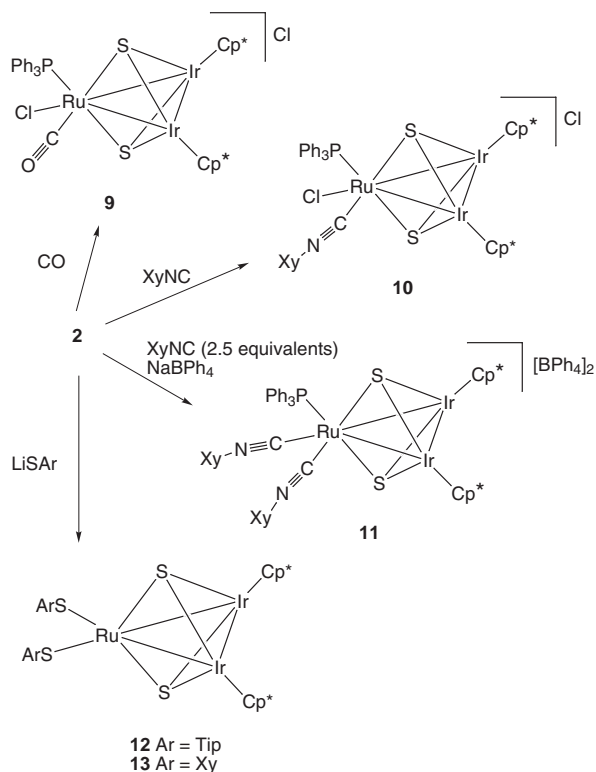**Table 4** Selected interatomic distances (Å) and angles (°) in complex 7

Ir(1)···Ir(2)	3.509(1)	Ir(1)–Ru(1)	2.830(2)
Ir(2)–Ru(1)	2.790(2)	Ir(1)–S(1)	2.336(6)
Ir(2)–S(2)	2.336(7)	Ir(2)–S(1)	2.315(7)
Ir(2)–S(2)	2.288(6)	Ru(1)–S(1)	2.413(6)
Ru(1)–S(2)	2.393(6)	Ru(1)–P(1)	2.236(6)
Ru(1)–P(2)	2.242(6)		
Ir(3)···Ir(4)	3.568(2)	Ir(3)–Ru(2)	2.793(2)
Ir(4)–Ru(2)	2.798(2)	Ir(3)–S(3)	2.314(7)
Ir(3)–S(4)	2.307(6)	Ir(4)–S(3)	2.350(6)
Ir(4)–S(4)	2.352(6)	Ru(2)–S(3)	2.420(6)
Ru(2)–S(4)	2.397(6)	Ru(2)–P(3)	2.242(6)
Ru(2)–P(4)	2.230(6)		
Ir(1)–Ru(1)–Ir(2)	77.26(6)	S(1)–Ir(1)–S(2)	78.9(2)
S(1)–Ir(2)–S(2)	80.4(2)	S(1)–Ru(1)–S(2)	76.3(2)
S(1)–Ru(1)–P(1)	98.4(2)	S(1)–Ru(1)–P(2)	176.5(2)
S(2)–Ru(1)–P(1)	170.2(2)	S(2)–Ru(1)–P(2)	101.1(2)
Ir(3)–Ru(2)–Ir(4)	79.31(6)	S(3)–Ir(3)–S(4)	79.6(2)
S(3)–Ir(4)–S(4)	77.9(2)	S(3)–Ru(2)–S(4)	75.8(2)
S(3)–Ru(2)–P(3)	101.3(2)	S(3)–Ru(2)–P(4)	172.7(2)
S(4)–Ru(2)–P(3)	173.4(2)	S(4)–Ru(2)–P(4)	98.4(2)

valence electrons of 7. As a related dihydrido cluster, we have recently synthesized [(Cp*Ru)$_2$(μ$_3$-S)$_2$(μ-H)RuH(PPh$_3$)$_2$] by treatment of [(Cp*Ru)$_2$(μ$_3$-S)$_2$(μ-H)RuCl(PPh$_3$)$_2$] with NaBH$_4$ and revealed its molecular structure with one terminal and one bridging hydrido ligand.[4c] In cluster 7 the large Ir–Ru–Ir angle probably enables both hydrido ligands to take bridging posi-tions without deforming the H–Ru–H moiety from the ideal linear geometry.

Ligand substitution reactions of cluster 2

In addition to the reactions with diphosphine ligands, cluster 2 underwent several ligand substitution reactions. Treatment with CO (1 atm) at room temperature gave the cationic carbonyl cluster [(Cp*Ir)$_2$(μ$_3$-S)$_2$RuCl(CO)(PPh$_3$)]Cl·0.5CH$_2$Cl$_2$ 9·0.5CH$_2$Cl$_2$ (Scheme 3). The ^{1}H NMR spectrum showed a broad singlet due to the Cp* ligands at δ 2.14, and the IR spectrum one strong absorption assigned to the ν(CO) at 1929 cm^{-1}. No further reaction with CO took place even after a long time. In contrast, when 2 was allowed to react with XyNC (Xy = 2,6-C$_6$H$_3$Me$_2$), stepwise ligand substitution was observed. Thus, treatment of 2 with 1 equivalent of XyNC afforded the mono-cationic cluster [(Cp*Ir)$_2$(μ$_3$-S)$_2$RuCl(CNXy)(PPh$_3$)]Cl 10, whereas the ^{1}H NMR analysis of the reaction mixture obtained

Scheme 3

Fig. 5 Molecular structure of complex **12·2C₆H₆**. Solvating benzene molecules and hydrogen atoms are omitted for clarity. Thermal ellipsoids are shown at the 50% probability level.

Table 5 Selected interatomic distances (Å) and angles (°) in complex **12·2C₆H₆**

Ir(1)–Ir(2)	2.7518(8)	Ir(1)–Ru(1)	2.976(1)
Ir(2)–Ru(1)	2.833(1)	Ir(1)–S(1)	2.283(4)
Ir(1)–S(2)	2.285(4)	Ir(2)–S(1)	2.275(5)
Ir(2)–S(2)	2.279(5)	Ru(1)–S(1)	2.223(4)
Ru(1)–S(2)	2.202(4)	Ru(1)–S(3)	2.276(3)
Ru(1)–S(4)	2.271(4)		
Ir(2)–Ir(1)–Ru(1)	59.14(3)	Ir(1)–Ir(2)–Ru(1)	64.38(3)
Ir(1)–Ru(1)–Ir(2)	56.48(3)	Ir(1)–Ru(1)–S(3)	123.69(10)
Ir(2)–Ru(1)–S(4)	92.7(1)	S(1)–Ir(1)–S(2)	84.7(1)
S(1)–Ir(2)–S(2)	85.0(1)	S(1)–Ru(1)–S(2)	88.1(1)
S(1)–Ru(1)–S(3)	134.5(2)	S(1)–Ru(1)–S(4)	107.9(2)
S(2)–Ru(1)–S(3)	122.0(2)	S(2)–Ru(1)–S(4)	118.9(2)
S(3)–Ru(1)–S(4)	87.8(1)		

by treatment of **2** with 2.5 equivalents of XyNC suggested that both of the chloro ligands in **2** were substituted by the XyNC ligands. Anion metathesis of the latter product with NaBPh₄ led to isolation of the dicationic cluster [(Cp*Ir)₂(μ₃-S)₂Ru-(CNXy)₂(PPh₃)][BPh₄]₂·CH₂Cl₂ **11·CH₂Cl₂**. Cluster **10** exhibited one IR band attributable to the v(CN) at 2054 cm⁻¹. On the other hand, two v(CN) bands were observed with cluster **11** at higher wavenumbers (2106 and 2135 cm⁻¹), reflecting its dicationic nature.

During the above reactions with CO and XyNC the PPh₃ ligand on the ruthenium atom in complex **2** remains intact. However, substitution of the two chloro ligands on the ruthenium centre by more bulky anionic ligands is expected to give co-ordinatively unsaturated clusters by sterically induced dissociation of the PPh₃ ligand. Actually, reactions of cluster **2** with lithium salts of sterically demanding 2,6-substituted arenethiolate anions such as TipS⁻ (Tip = 2,4,6-C₆H₂Pr$^i_3$) and XyS⁻ yielded [(Cp*Ir)₂(μ₃-S)₂Ru(SAr)₂] (Ar = Tip **12** or Xy **13**) (Scheme 3).

The molecular structure of complex **12·2C₆H₆** disclosed by X-ray diffraction study is illustrated in Fig. 5, and selected bond distances and angles are collected in Table 5. The trinuclear core with three metal–metal bonds and two μ₃-S ligands is retained. Although this cluster has 46 valence electrons and can be regarded as co-ordinatively unsaturated, the structure of the Ir₂Ru(μ₃-S)₂ core is very close to that of the 48e⁻ cluster **5** except that the Ru–(μ₃-S) bond distances in **12·2C₆H₆** [2.202(4), 2.223(4) Å] are shorter by 0.09–0.10 Å. The ruthenium atom is tetrahedrally co-ordinated by the four sulfur atoms, and the three metal atoms and the two sulfur atoms of the STip ligands are nearly coplanar. The two aromatic rings of the Tip groups are oriented almost perpendicular to this Ir₂RuS₂ plane (dihedral angles, 88.4 and 80.3°). Interestingly, the STip ligands are arranged in a highly unsymmetric conformation. Thus, the Tip group attached to the S(4) atom is directed away from the (Cp*Ir)₂(μ₃-S)₂ moiety, while that connected to the S(3) atom is located close to the Cp* ligand on the Ir(1) atom. At the same time, the Ir(1)–Ru(1)–S(3) angle [123.69(10)°] is significantly larger than the Ir(2)–Ru(1)–S(4) angle [92.7(1)°]. This charac-
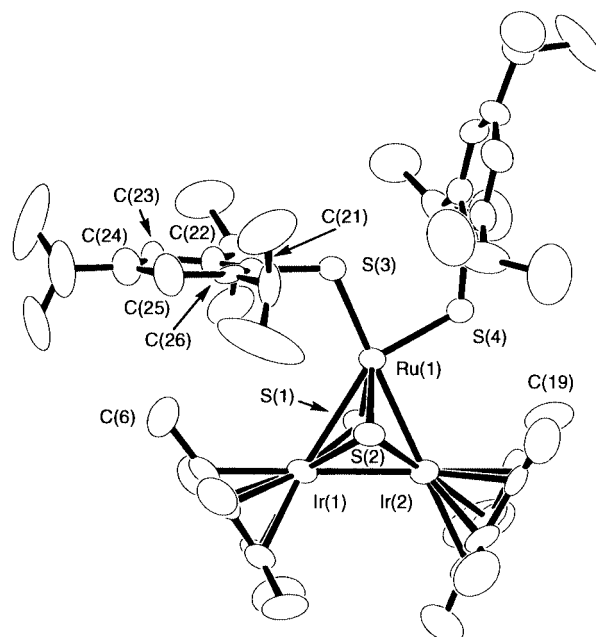
teristic conformation minimizes the steric congestion between the STip ligands and the Cp* ligands. In fact, unusually short non-bonding contacts are observed between the S(4) and C(19) (Cp* methyl) atoms (3.48 Å) and between the C(6) (Cp* methyl) atom and the C(21)–C(26) aromatic ring (3.43 Å), both of which are shorter than the sums of the van der Waals radii of a methyl group (2.0 Å) and a sulfur (1.85 Å) or aromatic carbon atom (1.7 Å).[16] In particular, the latter distance suggests the presence of an attractive interaction between the methyl group and the aromatic ring, *i.e.*, CH···π interaction.[17]

The ¹H NMR spectrum of complex **12** showed notable temperature dependence. At room temperature one broad signal at δ 1.99 attributable to Cp* ligands was observed, which split into two broad signals at δ 1.63 and 2.27 on cooling at −40 °C. This behavior can be accounted for by considering the conformational interchange of the STip ligands which are arranged in an unsymmetric structure as disclosed by the crystallographic study, eqn. (2).

(2)
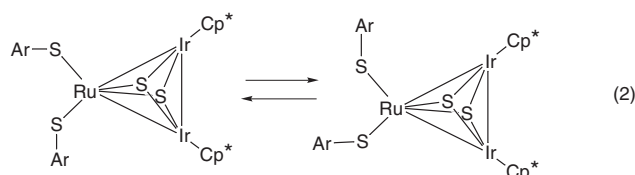
Conclusion

We have synthesized novel mixed-metal sulfido clusters **2**, **3** and **4** with the $Ir_2Ru(\mu_3\text{-}S)_2$ core by using the dinuclear hydrogen-sulfido complex **1** as the synthetic precursor. These clusters exhibited various reactivities including the regioselective alkylation of cluster **3** at either the ruthenium centre or the Cp* ligand. Clusters **5**, **6**, **7** and **8** have relatively labile or reactive ligands such as methyl, diene and hydrido ligands, and further reactions of these clusters as well as of the unsaturated clusters **12** and **13** are now under investigation.

Experimental

All manipulations were carried out under an atmosphere of nitrogen by the use of standard Schlenk tube techniques. Solvents were dried by common procedures and distilled before use. Complex **1**,[8a,b] $[RuH_2(PPh_3)_4]$,[18] $[RuCl_2(PPh_3)_3]$[19] and TipSH[20] were prepared according to literature methods. Lithium thiolates were prepared by reactions of Bu^nLi with the corresponding thiols. Other reagents were commercially obtained and used as received. The IR spectra were recorded on a Shimadzu 8100M spectrometer, ^1H (270 MHz) and $^{31}P\text{-}\{^1H\}$ NMR (109 MHz) spectra on a JEOL EX-270 spectrometer. Hydrogen gas evolution was determined by GLC analysis using a Shimadzu GC-8A gas chromatograph equipped with a molecular sieve 13X column. Elemental analyses were performed on a Perkin-Elmer 2400II CHN analyser. Amounts of the solvent molecules in the crystals were determined not only by elemental analyses but also by ^1H NMR spectroscopy.

Preparations

$[(Cp*Ir)_2(\mu_3\text{-}S)_2RuCl_2(PPh_3)]\cdot0.25thf$ 2·0.25thf. To a suspension of complex **1** (1.01 g, 1.28 mmol) in thf (30 cm³) was added $[RuH_2(PPh_3)_4]$ (1.75 g, 1.52 mmol), and the mixture stirred at room temperature for 20 h. The resulting dark brown solution was concentrated to 2 cm³, and the dark brown microcrystals deposited were collected by filtration and washed with hexane to give the trinuclear cluster **2·0.25thf** (1.36 g, 1.16 mmol, 91% yield) (Found: C, 40.09; H, 4.05. $C_{39}H_{47}Cl_2Ir_2O_{0.25}PRuS_2$ requires C, 39.99; H, 4.04%). δ_H(CDCl$_3$) 1.95 (30 H, s, Cp*), 7.28 (9 H, br, Ph) and 7.70 (6 H, br, Ph). δ_P(CDCl$_3$) 82.9 (br s). In a separate run the GLC analysis of the gaseous phase indicated that H_2 gas (1.44 mol per complex **1**) was evolved during the reaction.

$[(Cp*Ir)_2(\mu_3\text{-}S)_2RuCl(dppe)]Cl$ 3. To a suspension of complex **2·0.25thf** (2.00 g, 1.71 mmol) in thf (200 cm³) was added dppe (1.05 g, 2.64 mmol), and the mixture stirred at room temperature for 18 h. The resulting solution was concentrated to 10 cm³, and a dark brown powder deposited was collected by filtration and washed with diethyl ether to give **3** (1.96 g, 1.52 mmol, 89% yield) (Found: C, 42.64; H, 4.30. $C_{46}H_{54}Cl_2Ir_2$-P_2RuS_2 requires C, 42.85; H, 4.22%). δ_H(CDCl$_3$) 1.88 (30 H, s, Cp*), 2.25–2.40, 3.03–3.14 (2 H each, m, CH$_2$) and 7.15–7.84 (20 H, m, Ph). δ_P(CDCl$_3$) 81.0 (s).

$[(Cp*Ir)_2(\mu_3\text{-}S)_2RuCl(depe)]Cl$ 4. This complex was prepared from **2·0.25thf** and depe by a similar procedure to that described for **3** and isolated in 81% yield as a dark brown powder (Found: C, 32.78; H, 4.99. $C_{30}H_{54}Cl_2Ir_2P_2RuS_2$ requires C, 32.84; H, 4.96%). δ_H(CDCl$_3$) 1.06 [6 H, dt, ^3J(PH) 14.5, ^3J(HH) 7.6, CH$_2$*Me*], 1.27 [6 H, dt, ^3J(PH) 17.2, ^3J(HH) 7.6 Hz, CH$_2$*Me*], 1.43–1.54 (2 H, m, CH$_2$), 1.75–1.94 (6 H, m, CH$_2$), 1.98–2.16 (4 H, m, CH$_2$) and 2.11 (30 H, s, Cp*). δ_P(CDCl$_3$) 82.3 (s).

$[(Cp*Ir)_2(\mu_3\text{-}S)_2RuCl(depe)][BPh_4]$ 4′. To a suspension of complex **4** (50 mg, 0.046 mmol) in thf (10 cm³) was added NaBPh$_4$ (78 mg, 0.23 mmol), and the mixture stirred at room

temperature for 24 h. The solvent was removed *in vacuo*, and the residual solid extracted with CH$_2$Cl$_2$. The CH$_2$Cl$_2$ solution was concentrated to 5 cm³ and thf (0.3 cm³) added. Slow diffusion of hexane (10 cm³) into the solution afforded **4′** (6 mg, 0.004 mmol, 10% yield) as dark brown crystals (Found: C, 47.06; H, 5.53. $C_{54}H_{74}BClIr_2P_2RuS_2$ requires C, 46.96; H, 5.40%). δ_H(CDCl$_3$) 1.00 [6 H, dt, ^3J(PH) 14.5, ^3J(HH) 7.6, CH$_2$*Me*], 1.25 [6 H, dt, ^3J(PH) 17.2, ^3J(HH) 7.6, CH$_2$*Me*], 1.35–1.48 (2 H, m, CH$_2$), 1.66–1.90 (6 H, m, CH$_2$), 1.99 (30 H, s, Cp*), 2.05–2.12 (4 H, m, CH$_2$), 6.87 [4 H, t, ^3J(HH) 7.3, BPh$_4$], 7.03 [8 H, t, ^3J(HH) 7.4 Hz, BPh$_4$] and 7.38–7.44 (8 H, m, BPh$_4$). δ_P(CDCl$_3$) 82.3 (s).

$[(Cp*Ir)_2(\mu_3\text{-}S)_2RuMe(dppe)][PF_6]\cdot CH_2Cl_2$ 5·CH$_2$Cl$_2$. To a thf (20 cm³) solution of Me$_2$CuLi prepared from CuI (111 mg, 0.58 mmol) and MeLi (1.16 mmol, in ether) at −20 °C was added complex **3** (500 mg, 0.388 mmol) at this temperature, and the mixture kept at −20 °C for 1.5 h with stirring. Hexane (50 cm³) was added dropwise to the resulting dark brown mixture, and the dark brown powder precipitated was collected by filtration, washed with hexane and dried *in vacuo*. This crude product was dissolved in thf (30 cm³) and KPF$_6$ (714 mg, 3.88 mmol) added. The mixture was stirred at room temperature for 15 h and the solvent then removed *in vacuo*. The resulting dark brown solid was extracted with CH$_2$Cl$_2$. Addition of hexane to the concentrated CH$_2$Cl$_2$ solution afforded **5·CH$_2$Cl$_2$** (383 mg, 0.262 mmol, 67% yield) as dark brown crystals (Found: C, 39.28; H, 3.99. $C_{48}H_{59}Cl_2F_6Ir_2P_3RuS_2$ requires C, 39.39; H, 4.06%). δ_H(CDCl$_3$) −1.14 [3 H, t, ^3J(PH) 6.4 Hz, RuMe], 1.85 (30 H, s, Cp*), 2.12–2.34 (2 H, m, CH$_2$), 2.72–2.90 (2 H, m, CH$_2$) and 7.15–7.82 (20 H, m, Ph). δ_P(CDCl$_3$) 83.2 (s).

$[(Cp*Ir)\{(\eta^4\text{-}C_5Me_5CHCl_2)Ir\}(\mu_3\text{-}S)_2RuCl(dppe)]$ 6. To a thf (20 cm³) solution of CHCl$_2$Li prepared from CH$_2$Cl$_2$ (19 mg, 0.22 mmol) and Bu^{n}Li (0.22 mmol, in ether) at −78 °C was added complex **3** (100 mg, 0.078 mmol) at this temperature. The mixture was slowly warmed to room temperature with stirring. The solvent was evaporated to dryness, and the residual dark brown solid extracted with benzene. The benzene was removed *in vacuo*, and the residue dissolved in thf. Addition of hexane to the concentrated thf solution formed a small amount of dark brown crystals of **6** and a brown powder, the latter of which was filtered off. The brown filtrate was concentrated to give **6** (59 mg, 0.044 mmol, 57% yield) as dark brown microcrystals (Found: C, 42.59; H, 4.27. $C_{47}H_{55}Cl_3Ir_2P_2RuS_2$ requires C, 42.19; H, 4.14%). δ_H(C$_6$D$_6$) 1.21 (3 H, s, Me), 1.75 (15 H, s, Cp*), 1.79 (6 H, s, Me), 1.83–2.05 (2 H, m, CH$_2$), 1.95 (6 H, s, Me), 2.86–3.08 (2 H, m, CH$_2$), 5.23 (1 H, s, CHCl$_2$) and 7.00–8.21 (20 H, m, Ph). δ_P(C$_6$D$_6$) 81.0 (s).

$[(Cp*Ir)_2(\mu_3\text{-}S)_2(\mu\text{-}H)_2Ru(dppe)]$ 7. To a solution of complex **3** (499 mg, 0.387 mmol) in CH$_2$Cl$_2$ (30 cm³)–ethanol (70 cm³) was added NaBH$_4$ (101 mg, 2.67 mmol) in small portions, and the mixture stirred at room temperature for 45 h. The resulting dark brown solution was evaporated to dryness, and the residue extracted with benzene. The benzene was removed *in vacuo* and the dark brown residue recrystallized from thf–hexane to give **7** (198 mg, 0.162 mmol, 42% yield) as a dark brown powder (Found: C, 45.52; H, 4.79. $C_{46}H_{56}Ir_2P_2RuS_2$ requires C, 45.27; H, 4.62%). δ_H(C$_6$D$_6$) −14.73 [2 H, t, ^2J(PH) 13.4, hydrido], 1.97 (30 H, s, Cp*), 2.78 [4 H, d, ^2J(PH) 17.8 Hz, CH$_2$] and 7.02–7.73 (20 H, m, Ph). δ_P(C$_6$D$_6$) 73.6 (s).

$[(Cp*Ir)_2(\mu_3\text{-}S)_2(\mu\text{-}H)_2Ru(depe)]$ 8. To a solution of complex **4** (200 mg, 0.182 mmol) in CH$_2$Cl$_2$ (10 cm³)–ethanol (5 cm³) was added NaBH$_4$ (69 mg, 1.8 mmol) in small portions, and the mixture stirred at room temperature for 16 h. The resulting dark brown solution was evaporated to dryness and the residue extracted with hexane. Evaporation of the solvent to dryness gave essentially pure **8** (100 mg, 0.097 mmol, 53% yield) as a

Table 6 X-Ray crystallographic data for complexes **4′**, **5·CH₂Cl₂**, **6**, **7** and **12·2C₆H₆**

	4′	**5·CH₂Cl₂**	**6**	**7**	**12·2C₆H₆**
Formula	C₅₄H₇₄BClIr₂P₂RuS₂	C₄₈H₅₉Cl₂F₆Ir₂P₃RuS₂	C₄₇H₅₅Cl₃Ir₂P₂RuS₂	C₄₆H₅₆Ir₂P₂RuS₂	C₆₂H₈₈Ir₂RuS₄
M	1381.02	1463.44	1337.89	1220.53	1447.13
Crystal system	Monoclinic	Monoclinic	Monoclinic	Monoclinic	Monoclinic
Space group	$P2_1/a$	$P2_1/n$	$P2_1/c$	$P2_1$	$P2_1$
$a/Å$	17.451(3)	11.460(3)	12.287(2)	17.369(2)	12.081(2)
$b/Å$	17.774(4)	12.065(4)	15.247(2)	14.609(1)	16.767(3)
$c/Å$	17.776(3)	37.612(3)	25.921(2)	17.631(4)	15.752(2)
$β/°$	97.66(1)	94.31(2)	94.10(1)	90.26(1)	91.66(1)
$U/Å^3$	5464(1)	5185(2)	4843(1)	4473(1)	3189.4(8)
Z	4	4	4	4	2
$μ$(Mo-Kα)/cm⁻¹	53.63	57.52	61.54	64.80	45.73
Independent reflections	12549	9033	8528	10679	5825
	($R_{int} = 0.046$)	($R_{int} = 0.043$)	($R_{int} = 0.029$)	($R_{int} = 0.043$)	($R_{int} = 0.025$)
Final R, R' [$I > 3.0σ(I)$]	0.048, 0.032	0.041, 0.042	0.038, 0.025	0.057, 0.039	0.041, 0.027

dark brown powder (Found: C, 35.39; H, 5.47. C₃₀H₅₆Ir₂P₂RuS₂ requires C, 35.04; H, 5.49%). $δ_H$(C₆D₆) −14.56 [2 H, t, ^2J(PH) 15.9, hydrido], 1.10 [12 H, dt, ^3J(PH) 14.7, ^3J(HH) 7.6 Hz, CH₂*Me*], 1.59–1.80 (12 H, m, CH₂) and 2.07 (30 H, s, Cp*). $δ_P$(C₆D₆) 79.6 (s).

[(Cp*Ir)₂(μ₃-S)₂RuCl(CO)(PPh₃)]Cl·0.5CH₂Cl₂ 9·0.5CH₂Cl₂. A CH₂Cl₂ (5 cm³) solution of complex **2·0.25thf** (49 mg, 0.042 mmol) was stirred under an atmosphere of CO at room temperature for 2 h. Then the solution was concentrated under reduced pressure, and hexane added to the resultant solution to give **9·0.5CH₂Cl₂** (42 mg, 0.034 mmol, 82% yield) as dark red needles (Found: C, 38.50; H, 4.00. C₃₉.₅H₄₆Cl₃Ir₂OPRuS₂ requires C, 38.77; H, 3.79%). $δ_H$(CDCl₃) 2.14 (30 H, s, Cp*) and 7.40–7.57 (15 H, m, Ph). $δ_P$(CDCl₃) 40.5 (s). $\tilde{ν}_{max}$/cm⁻¹ (CO) 1929 (KBr).

[(Cp*Ir)₂(μ₃-S)₂RuCl(CNXy)(PPh₃)]Cl 10. A mixture of complex **2·0.25thf** (93 mg, 0.079 mmol) and XyNC (11 mg, 0.083 mmol) in CH₂Cl₂ (5 cm³) was stirred at room temperature for 20 h. The reaction mixture was filtered and concentrated under reduced pressure. Addition of hexane to the concentrated solution afforded **10** (82 mg, 0.064 mmol, 80% yield) as a dark brown solid (Found: C, 43.58; H, 4.24; N, 0.84. C₄₇H₅₄Cl₂-Ir₂NPRuS₂ requires C, 43.95; H, 4.24; N, 1.09%). $δ_H$(CDCl₃) 2.05 (6 H, s, *o*-Me), 2.11 (30 H, s, Cp*), 7.00 (3 H, br, Ar) and 7.34–7.53 (15 H, m, PPh₃). $δ_P$(CDCl₃) 43.0 (s). $\tilde{ν}_{max}$/cm⁻¹ (CN) 2054 (KBr).

[(Cp*Ir)₂(μ₃-S)₂Ru(CNXy)₂(PPh₃)][BPh₄]₂·CH₂Cl₂ 11·CH₂Cl₂. A mixture of complex **2·0.25thf** (100 mg, 0.085 mmol), XyNC (28 mg, 0.21 mmol) and NaBPh₄ (292 mg, 0.853 mmol) in CH₂Cl₂ (5 cm³) was stirred at room temperature for 15 h. The reaction mixture was filtered and concentrated, and addition of ether afforded **11·CH₂Cl₂** (111 mg, 0.054 mmol, 63% yield) as a reddish brown powder (Found: C, 61.03; H, 5.10; N, 1.57. C₁₀₅H₁₀₅B₂Cl₂Ir₂N₂PRuS₂ requires C, 60.98; H, 5.12; N, 1.35%). $δ_H$(CD₂Cl₂) 1.91 (30 H, s, Cp*), 2.04 (12 H, s, *o*-Me) and 6.80–7.51 (61 H, m, Ar). $δ_P$(CD₂Cl₂) 45.0 (s). $\tilde{ν}_{max}$/cm⁻¹ (CN) 2106 and 2135 (KBr).

[(Cp*Ir)₂(μ₃-S)₂Ru(STip)₂] 12. A mixture of complex **2·0.25thf** (102 mg, 0.087 mmol) and LiSTip (83 mg, 0.34 mmol) in thf (8 cm³) was stirred at room temperature for 15 h. Then the solvent was evaporated to dryness, and the residue extracted with benzene. Addition of MeOH to the concentrated benzene solution afforded crystals of **12·2C₆H₆** which were used for crystallographic study. The crystals gave off benzene on drying under vacuum to give **12** (78 mg, 0.060 mmol, yield 69%) as a dark brown solid (Found: C, 46.43; H, 6.01. C₅₀H₇₆Ir₂RuS₄ requires C, 46.52; H, 5.93%). $δ_H$(CDCl₃) 1.13 [24 H, d, ^3J(HH) 6.9, *o*-CH*Me*₂], 1.19 [12 H, d, ^3J(HH) 6.9, *p*-CH*Me*₂], 1.99 (30

H, br s, Cp*), 2.71 [2 H, sep, ^3J(HH) 6.9, *p*-C*H*Me₂], 3.85 [4 H, sep, ^3J(HH) 6.9 Hz, *o*-C*H*Me₂] and 6.75 (4 H, s, Ar).

[(Cp*Ir)₂(μ₃-S)₂Ru(SXy)₂] 13. A mixture of complex **2·0.25thf** (104 mg, 0.089 mmol) and LiSXy (56 mg, 0.39 mmol) in thf (8 cm³) was stirred at room temperature for 15 h. The solvent was evaporated to dryness and the residue extracted with thf. Addition of hexane to the concentrated thf solution afforded **13** (10 mg, 0.009 mmol, 10% yield) as dark brown plates (Found: C, 39.86; H, 4.61. C₃₆H₄₈Ir₂RuS₄ requires C, 39.50; H, 4.42%). $δ_H$(CDCl₃) 1.97 (30 H, br s, Cp*), 2.17 (12 H, br, *o*-Me) and 6.90 (6 H, br, Ar).

Crystallography

Crystallographic data for complexes **4′**, **5·CH₂Cl₂**, **6**, **7** and **12·2C₆H₆** are summarized in Table 6. Diffraction data were collected on a Rigaku AFC7R four-circle automated diffractometer at 294 K with graphite-monochromatized Mo-Kα radiation (λ = 0.71069 Å) using the ω–2θ scan technique for **4′**, **7** and **12·2C₆H₆** and the ω scan technique for **5·CH₂Cl₂** and **6**.

The structure solution and refinements were carried out by using the TEXSAN crystallographic software package.[21] The positions of the non-hydrogen atoms were determined by Patterson methods (DIRDIF PATTY[22]) and subsequent Fourier syntheses. All non-hydrogen atoms were refined by full-matrix least-squares techniques (based on F) with anisotropic thermal parameters except for the carbon atoms of the CH₂Cl₂ molecule in **5·CH₂Cl₂**, cluster **7** and the C₆H₆ molecules in **12·2C₆H₆**. The carbon atoms of **7** were refined with isotropic parameters, while fixed parameters were used for the carbon atoms of the solvent molecules in **5·CH₂Cl₂** and **12·2C₆H₆**. Hydrogen atoms except for those of the CH₂Cl₂ molecule in **5·CH₂Cl₂** and the hydrido ligands in **7** were placed at calculated positions ($d_{C-H} = 0.95$ Å) and included with fixed isotropic parameters. For **7** and **12·2C₆H₆**, the Flack absolute structure parameters[23] were close to zero [−0.02(2) and −0.01(2)].

CCDC reference number 186/1523.

See http://www.rsc.org/suppdata/dt/1999/2575/ for crystallographic files in .cif format.

References

1 R. H. Holm, S. Ciurli and J. A. Weigel, *Prog. Inorg. Chem.*, 1990, **38**, 1; B. Krebs and G. Henkel, *Angew. Chem., Int. Ed. Engl.*, 1991, **30**, 769; T. Shibahara, *Coord. Chem. Rev.*, 1993, **123**, 73; T. Saito, in *Early Transition Metal Clusters with π-Donor Ligands*, ed. M. H.

Chisholm, VCH, New York, 1995, ch. 3; I. Dance and K. Fisher, *Prog. Inorg. Chem.*, 1994, **41**, 637; P. Mathur, *Adv. Organomet. Chem.*, 1997, **41**, 243; H. Ogino, S. Inomata and H. Tobita, *Chem. Rev.*, 1998, **98**, 2093.

2 D. Coucouvanis, in *Molybdenum Enzymes, Cofactors, and Model Systems*, eds. E. I. Stiefel, D. Coucouvanis and W. E. Newton, American Chemical Society, Washington, DC, 1993, p. 304; J. B. Howard and D. C. Rees, *Chem. Rev.*, 1996, **96**, 2965; B. K. Burgess and D. J. Lowe, *Chem. Rev.*, 1996, **96**, 2983; D. Sellmann and J. Sutter, *Acc. Chem. Res.*, 1997, **30**, 460.

3 R. A. Sánchez-Delgado, *J. Mol. Catal.*, 1994, **86**, 287; C. Bianchini and A. Meli, *J. Chem. Soc.*, *Dalton Trans.*, 1996, 801; M. D. Curtis and S. H. Druker, *J. Am. Chem. Soc.*, 1997, **119**, 1027; C. Bianchini and A. Meli, *Acc. Chem. Res.*, 1998, **31**, 109.

4 (*a*) M. Hidai, Y. Mizobe and H. Matsuzaka, *J. Organomet. Chem.*, 1994, **473**, 1; (*b*) M. Hidai and Y. Mizobe, *ACS Symp. Ser.*, 1996, **653**, 310; (*c*) S. Kuwata, M. Andou, K. Hashizume, Y. Mizobe and M. Hidai, *Organometallics*, 1998, **17**, 3429; (*d*) S. Kuwata and M. Hidai, *Chem. Lett.*, 1998, 885; (*e*) Z. Tang, Y. Nomura, S. Kuwata, Y. Ishii, Y. Mizobe and M. Hidai, *Inorg. Chem.*, 1998, **37**, 4909; (*f*) J.-P. Qü, D. Masui, Y. Ishii and M. Hidai, *Chem. Lett.*, 1998, 1003; (*g*) Y. Mizobe, M. Hosomizu and M. Hidai, *Inorg. Chim. Acta*, 1998, **273**, 238; (*h*) T. Ikada, S. Kuwata, Y. Mizobe and M. Hidai, *Inorg. Chem.*, 1998, **37**, 5793; (*i*) S. Takemoto, S. Kuwata, Y. Nishibayashi and M. Hidai, *Inorg. Chem.*, 1998, **37**, 6428; (*j*) T. Sato, M. Nishio, Y. Ishii, H. Yamazaki and M. Hidai, *J. Organomet. Chem.*, 1998, **569**, 99; (*k*) T. Ikada, S. Kuwata, Y. Mizobe and M. Hidai, *Inorg. Chem.*, 1999, **38**, 64.

5 H. Matsuzaka, Y. Takagi and M. Hidai, *Organometallics*, 1994, **13**, 13; H. Matsuzaka, Y. Takagi, Y. Ishii, M. Nishio and M. Hidai, *Organometallics*, 1995, **14**, 2153; H. Shimada, J.-P. Qü, H. Matsuzaka, Y. Ishii and M. Hidai, *Chem. Lett.*, 1995, 671; Y. Nishibayashi, Y. Yamanashi, Y. Takagi and M. Hidai, *Chem. Commun.*, 1997, 859; Y. Takagi, H. Matsuzaka, Y. Ishii and M. Hidai, *Organometallics*, 1997, **16**, 4445.

6 T. Murata, H. Gao, Y. Mizobe, F. Nakano, S. Motomura, T. Tanase, S. Yano and M. Hidai, *J. Am. Chem. Soc.*, 1992, **114**, 8287; T. Murata, Y. Mizobe, H. Gao, Y. Ishii, T. Wakabayashi, F. Nakano, T. Tanase, S. Yano, M. Hidai, I. Echizen, H. Nanikawa and S. Motomura, *J. Am. Chem. Soc.*, 1994, **116**, 3389; T. Wakabayashi, Y. Ishii, T. Murata, Y. Mizobe and M. Hidai, *Tetrahedron Lett.*, 1995, **36**, 5585; T. Wakabayashi, Y. Ishii, K. Ishikawa and M. Hidai, *Angew. Chem.*, *Int. Ed. Engl.*, 1996, **35**, 2123.

7 K. Hashizume, Y. Mizobe and M. Hidai, *Organometallics*, 1996, **15**, 3303.

8 (*a*) Z. Tang, Y. Nomura, Y. Ishii, Y. Mizobe and M. Hidai, *Organometallics*, 1997, **16**, 151; (*b*) Z. Tang, Y. Nomura, Y. Ishii, Y. Mizobe and M. Hidai, *Inorg. Chim. Acta*, 1998, **267**, 73; (*c*) D. Masui, Y. Ishii and M. Hidai, *Chem. Lett.*, 1998, 717.

9 C. K. Johnson, ORTEP II, Report ORNL-5138, Oak Ridge National Laboratory, Oak Ridge, TN, 1976.

10 A. Fumagalli, F. Demartin and A. Sironi, *J. Organomet. Chem.*, 1985, **279**, C33; D. Mani and H. Vahrenkamp, *Chem. Ber.*, 1986, **119**, 3649; H. Jungbluth, G. Süss-Fink, M. A. Pellinghelli and A. Tiripicchio, *Organometallics*, 1990, **9**, 1670; D. Carmona, J. Ferrer, A. Mendoza, F. J. Lahoz, J. Reyes and L. A. Oro, *Angew. Chem.*, *Int. Ed. Engl.*, 1991, **30**, 1171; G. Süss-Fink, S. Haak, V. Ferrand and H. Stoeckli-Evans, *J. Chem. Soc.*, *Dalton Trans.*, 1997, 3861; A. U. Härkönen, M. Ahlgrén, T. A. Pakkanen and J. Pursiainen, *Organometallics*, 1997, **16**, 689; V. Ferrand, G. Süss-Fink, A. Neels and H. Stoeckli-Evans, *J. Chem. Soc.*, *Dalton Trans.*, 1998, 3825; A. U. Härkönen, M. Ahlgrén, T. A. Pakkanen and J. Pursiainen, *J. Organomet. Chem.*, 1999, **573**, 225.

11 (*a*) A. M. Mueting, P. D. Boyle, R. Wagner and L. H. Pignolet, *Inorg. Chem.*, 1988, **27**, 271; (*b*) T. A. Bright, R. A. Jones, S. U. Koschmieder and C. M. Nunn, *Inorg. Chem.*, 1988, **27**, 3819; (*c*) A. Venturelli and T. B. Rauchfuss, *J. Am. Chem. Soc.*, 1994, **116**, 4824; (*d*) T. Nishioka and K. Isobe, *Chem. Lett.*, 1994, 1661; (*e*) W. D. Jones and R. M. Chin, *J. Am. Chem. Soc.*, 1994, **116**, 198; (*f*) D. A. Vicic and W. D. Jones, *Organometallics*, 1997, **16**, 1912.

12 J. R. Lockemeyer, T. B. Rauchfuss and A. L. Rheingold, *J. Am. Chem. Soc.*, 1989, **111**, 5733; K. Hashizume, Y. Mizobe and M. Hidai, *Organometallics*, 1995, **14**, 5367.

13 For example, (*a*) K. Moseley, J. W. Kang and P. M. Maitlis, *J. Chem. Soc. A*, 1970, 2875; (*b*) H. Werner, B. Heiser, B. Klingert and R. Dülfel, *J. Organomet. Chem.*, 1982, **240**, 179; (*c*) K. Tanaka, Y. Kushi, K. Tsuge, K. Toyohara, T. Nishioka and K. Isobe, *Inorg. Chem.*, 1998, **37**, 120.

14 H. Werner, *Angew. Chem.*, *Int. Ed. Engl.*, 1983, **22**, 927.

15 W. E. Watts, in *Comprehensive Organometallic Chemistry*, eds. G. Wilkinson, F. G. A. Stone and E. W. Abel, Pergamon, London, 1982, vol. 8, p. 1013.

16 L. Pauling, in *The Nature of the Chemical Bond*, 3rd edn., Cornell University Press, Ithaca, NY, 1960; A. Bondi, *J. Phys. Chem.*, 1964, **68**, 441.

17 M. Nishio and M. Hirota, *Tetrahedron*, 1989, **45**, 7201; M. Nishio, Y. Umezawa, M. Hirota and Y. Takeuchi, *Tetrahedron*, 1995, **51**, 8665.

18 R. O. Harris, N. K. Hota, L. Sadavoy and J. M. C. Yuen, *J. Organomet. Chem.*, 1973, **54**, 259.

19 P. S. Hallman, T. A. Stephenson and G. Wilkinson, *Inorg. Synth.*, 1972, **12**, 237.

20 P. J. Blower, J. R. Dilworth, J. P. Hutchinson and J. A. Zubieta, *J. Chem. Soc.*, *Dalton Trans.*, 1985, 1533.

21 TEXSAN, Crystal Structure Analysis Package, Molecular Structure Corp., The Woodlands, TX, 1985 and 1992.

22 PATTY, P. T. Beurskens, G. Admiraal, G. Beurskens, W. P. Bosman, S. Garcia-Granda, R. O. Gould, J. M. M. Smits and C. Smykalla, The DIRDIF program system, Technical Report of the Crystallography Laboratory, University of Nijmegen, 1992.

23 H. D. Flack, *Acta Crystallogr.*, *Sect. A*, 1983, **39**, 876.

Paper 9/02999K